IEEE Access
Multidisciplinary | Rapid Review | Open Access Journal

Received 5 September 2022, accepted 10 September 2022, date of publication 12 September 2022,
date of current version 21 September 2022.

Digital Object Identifier 10.1109/ACCESS.2022.3206381

RESEARCH ARTICLE

Novel Self-Excited Brush-Less Wound Field Vernier Machine Topology

SYED SABIR HUSSAIN BUKHARI[1], JUNAID IKRAM[2], FENGXIANG WANG[3], (Senior Member, IEEE), XINHONG YU[3], (Senior Member, IEEE), JUNAID IMTIAZ[4], (Member, IEEE), JORGE RODAS[5], (Senior Member, IEEE), AND JONGSUK RO[6,7]

[1]Department of Electrical Engineering, Sukkur IBA University, Sukkur, Sindh 65200, Pakistan
[2]Department of Electrical and Computer Engineering, COMSATS University Islamabad, Islamabad 45550, Pakistan
[3]National and Local Joint Engineering Research Center for Electrical Drives and Power Electronics, Quanzhou Institute of Equipment Manufacturing, Haixi Institute, Chinese Academy of Sciences, Quanzhou, Fujian 362216, China
[4]Department of Electrical Engineering, Bahria University, Islamabad 44000, Pakistan
[5]Laboratory of Power and Control Systems (LSPyC), Facultad de Ingeniería, Universidad Nacional de Asunción, Luque 2060, Paraguay
[6]School of Electrical and Electronics Engineering, Chung-Ang University, Seoul 06910, South Korea
[7]Department of Intelligent Energy and Industry, Chung-Ang University, Seoul 06910, South Korea

Corresponding author: Jongsuk Ro (jongsukro@gmail.com)

This work was supported in part by the National Research Foundation of Korea (NRF) funded by the Ministry of Science and ICT under Grant NRF-2022R1A2C2004874, and in part by the Brain Pool (BP) Program through the National Research Foundation (NRF) of Korea funded by the Ministry of Science and ICT under Grant 2019H1D3A1A01102988.

ABSTRACT To realize the brush-less operation for wound field vernier machines (WFVMs), a novel self-excited topology is proposed in this paper which involves a four-pole main armature winding and a two-pole excitation winding connected in series using an uncontrolled rectifier. Upon supplying current from a single current-controlled voltage source inverter (VSI), this procedure results in four-pole and two-pole magnetomotive force (MMF) components in the airgap. The four-pole MMF produces the main stator field while the two-pole MMF component develops a sub-harmonic field in the airgap. The rotor is altered to house a forty-four-pole rotor field and two-pole harmonic windings. The two-pole harmonic field is employed to induce a current in the harmonic winding, which is rectified by means of a full-bridge diode rectifier to energize the rotor field winding and realize brush-less operation for WFVM. Two-dimensional finite element analysis (2-D FEA) is implemented in JMAG-Designer to confirm the operation of the proposed WFVM topology and attain the electromagnetic performance for a four-pole, twenty-four-slot outer-rotor vernier machine.

INDEX TERMS Wound field vernier machine, harmonic field excitation, self-excited machines, wound rotor.

I. INTRODUCTION

In regular electric drive systems, the mechanical gearing systems are generally used to achieve the speed/torque difference between the high-speed motor and the low-speed prime-mover shafts. Mechanical gearing systems are noisy and lead to high maintenance costs. Furthermore, these gearing systems encounter lifetime challenges as their life span is usually shorter than electromechanical systems whereas the direct-drive systems operating at low-speed and high-torque conditions result in substantially large machines because of a large number of rotor poles [1].

In the 1960s, a new machine that uses the magnetic gearing phenomenon caused by flux modulation was developed. This machine is known as the vernier machine (VM) and has received much attention over the last couple of decades because of the progress in permanent magnets (PMs) development technology. It is because the vernier PM machines can generate two-to-three times the output torque in comparison with the conventional PM machines of the same

The associate editor coordinating the review of this manuscript and approving it for publication was Atif Iqbal.

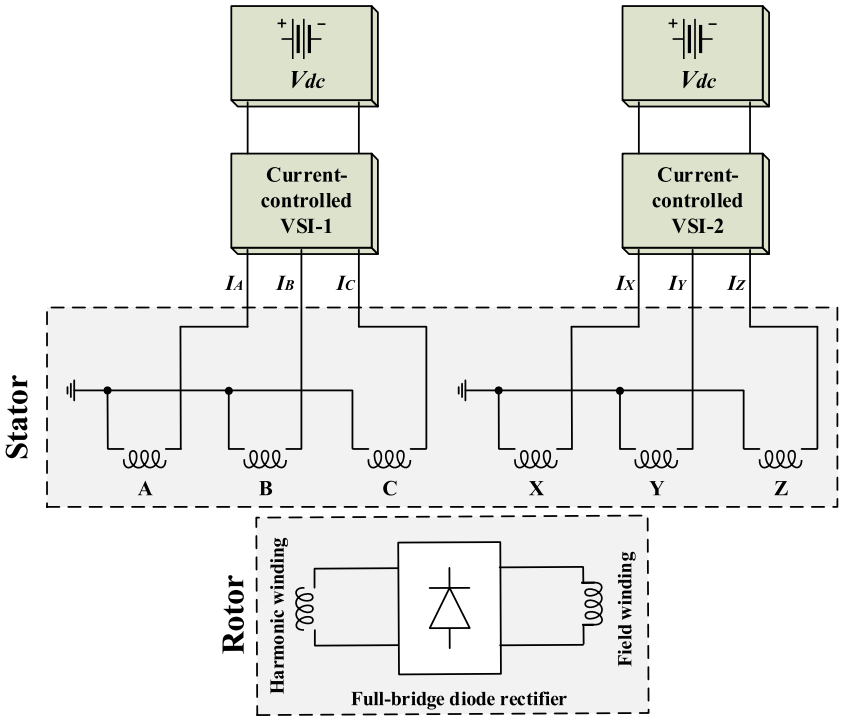

FIGURE 1. Conventional brush-less WFVM topology proposed in [6].

volume [2], [3]. Furthermore, these machines do not require any mechanical gearing system, which reduces their noise and maintenance costs. As a consequence of these advantages, PM vernier machines (PMVMs) are considered an essential potential enabler for wind power generators and ship propulsion applications. In addition, the torque ripple of vernier PM machines is relatively low, which is a feature of significant importance for reducing the noise and vibration of the machine system while considering the wave energy extraction, in-wheel motors, auto-focusing lens, and free-piston generator applications [4].

To realize the low-speed operation incorporated with the gearing effect, the PMVMs require a large number of rotor magnet poles which increases the cost of the machine system. It is because the price of the rare-earth materials needed for the development of PMs is increasing over time which also causes poor stability and reliability problems. Also, the mining of rare-earth materials inevitably leads to serious environmental issues. Notably, the price of Nd-Fe-B magnets in 2005 was U.S. $250/kg which increased to U.S. $437/kg in 2012 [5], [6], [7], [8], [9], [10], [11].

The reluctance vernier machines (RVMs) are the least expensive in comparison with PMVMs as they do not require any PM for the rotor field excitation; however, these machines suffer from low torque density [2].

On the other hand, wound field vernier machines (WFVMs) address the high cost and low torque density concerns associated with PMVMs and RVMs, respectively. However, these machines require brushes and slip-rings for the energization of the rotor field winding, which raises the maintenance cost of the machine system. This encouraged researchers to explore different brush-less topologies of WFVMs.

The conventional brush-less WFVM topologies require exciters and pilot-exciters for their rotor field excitation. Exciters and pilot-exciters are small-sized electrical machines fitted on the shaft of the WFVM machine to realize brush-less operation through the electromagnetic induction phenomenon; however, these small-sized machines enhance the overall cost and size of the machine system. Therefore, these brush-less WFVM topologies could not get considerable attention in the market [12], [13], [14].

Recently, researchers have started investigating different brush-less topologies for the wound rotor synchronous machines whose rotor field is energized through the harmonic field excitation method. In principle, the harmonic field excitation method involves developing a supplementary harmonic MMF component in the airgap besides the fundamental component [15], [17], [18]. In the case of WFVMs, the only successful attempt in this regard is recently made in which a brush-less WFVM topology for electric vehicle and washing machine applications while considering the sub-harmonic field excitation method is developed [19]. This topology is based on a dual-inverter-outline. The armature winding is split up into two halves (ABC and XYZ), each of which is having a different star connection, and is supplied current (I_{ABC} and I_{XYZ}) from a designated inverter, namely current-controlled VSI-1, and VSI-2. The frequency of the output inverter currents is the same; however, the magnitude of currents is different. This procedure generates the fundamental and sub-harmonic MMF components in the airgap. The fundamental MMF develops the main stator field, while

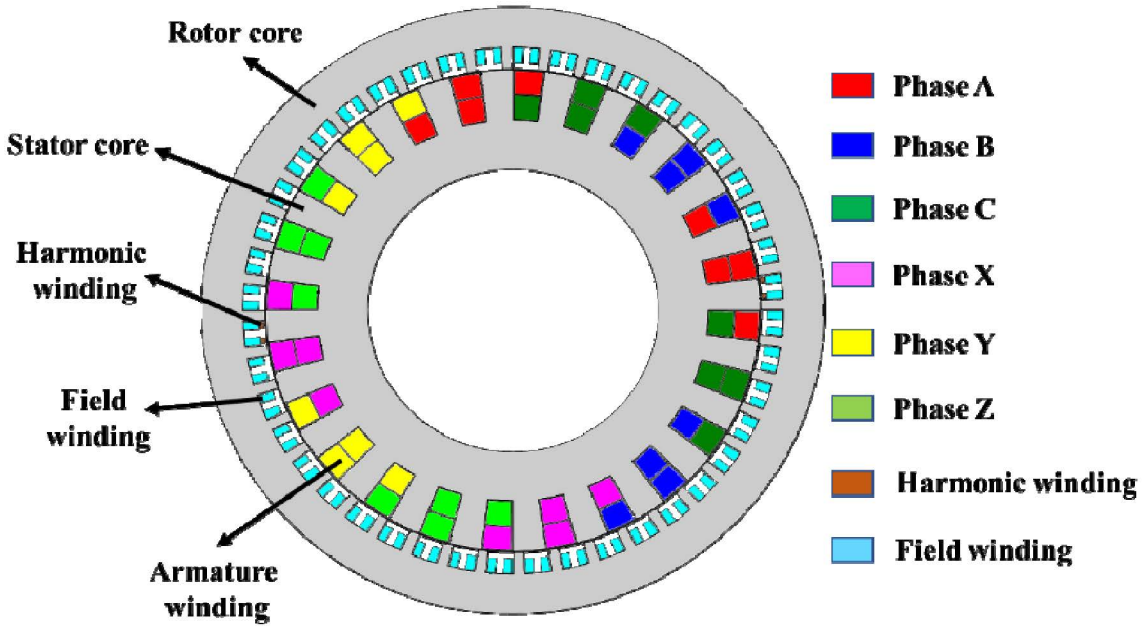

FIGURE 2. Machine used for the validation of the conventional brush-less WFVM topology proposed in [6].

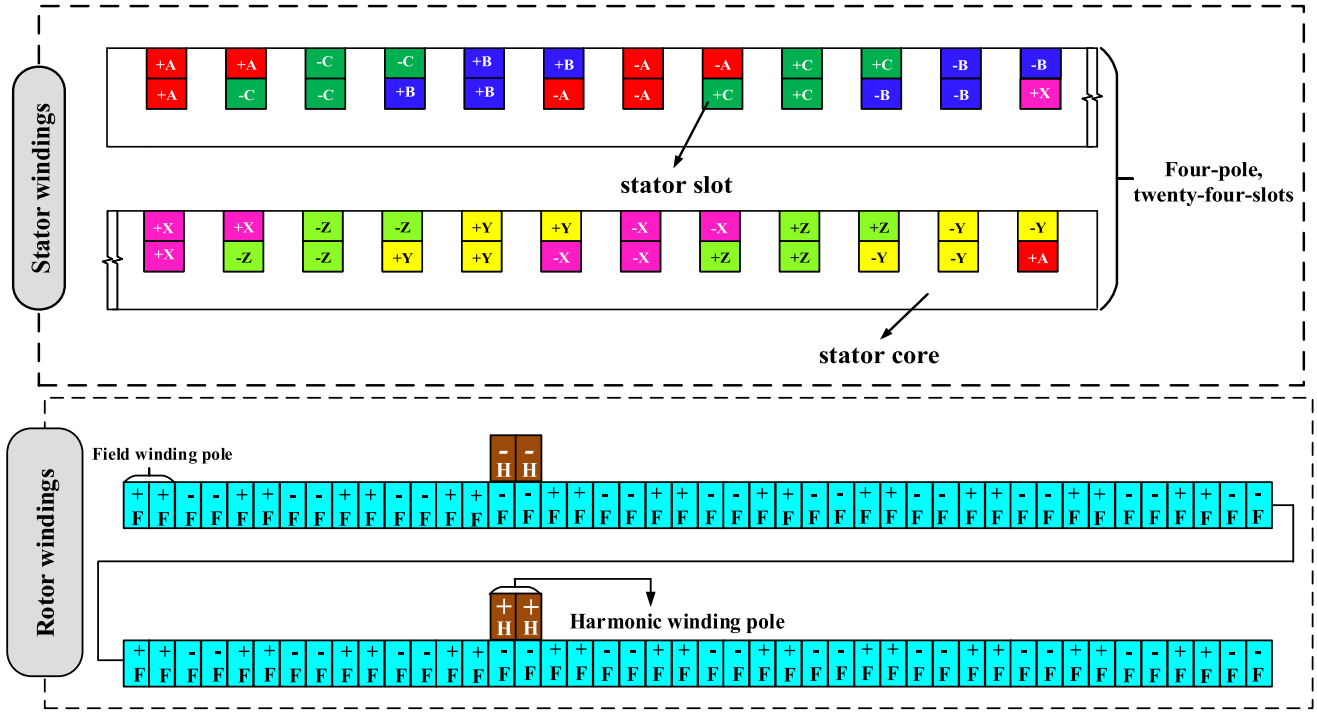

FIGURE 3. Armature and rotor winding outline used for the validation of the conventional brush-less WFVM topology proposed in [6].

the sub-harmonic MMF component induces a current in the harmonic winding which is rectified to energize the rotor field winding of the WFVM to realize its brush-less operation. This topology was implemented for a four-pole, twenty-four-slot vernier machine. The proposed brush-less topology is presented in Fig. 1, whereas the employed machine as well as its stator and rotor winding outlines are presented in Fig. 2 and 3, respectively. Although this topology achieved the brush-less operation for WFVMs, the usage of a dual-inverter-outline makes it expensive and increases its overall size. In addition, it exhibits some performance issues such as low average torque, high losses, and low efficiency because of the different magnitude of current flowing in two halves of the armature winding [20], [21], [22], [23].

This paper proposes a new self-excited brush-less WFVM topology, which employs a four-pole main armature winding and a two-pole excitation winding connected in series by means of an uncontrolled rectifier. As the machine is

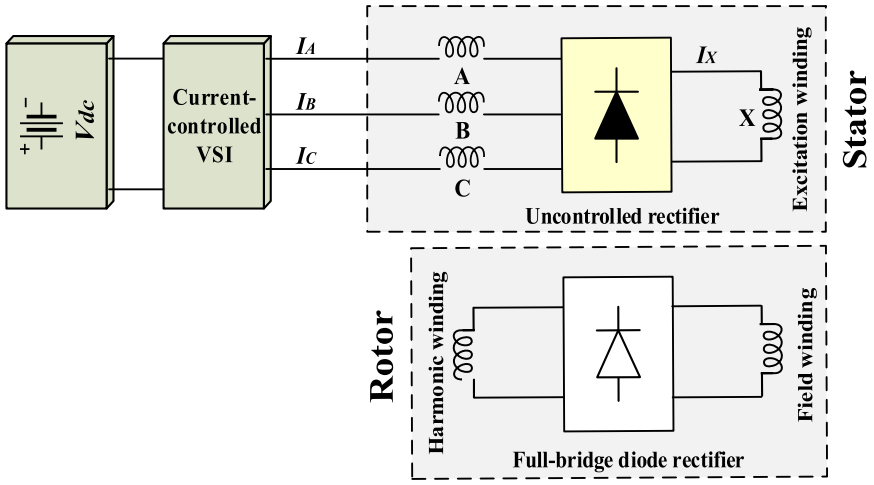

FIGURE 4. Proposed self-excited brush-less WFVM topology.

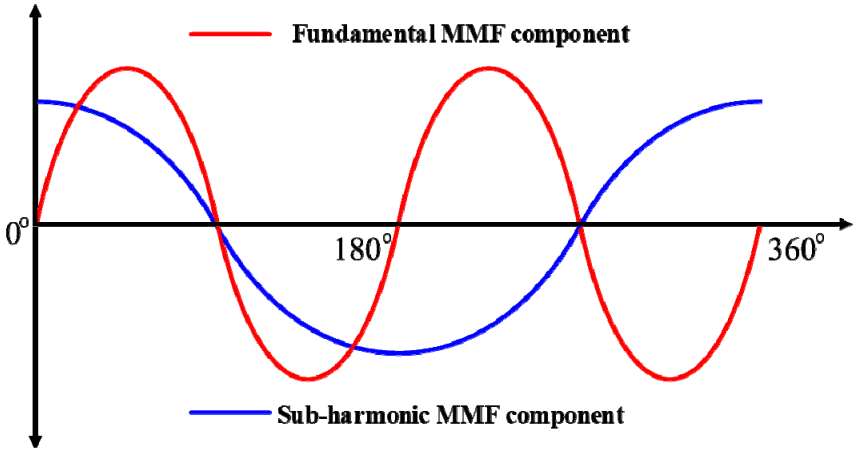

FIGURE 5. MMF components generated in the airgap.

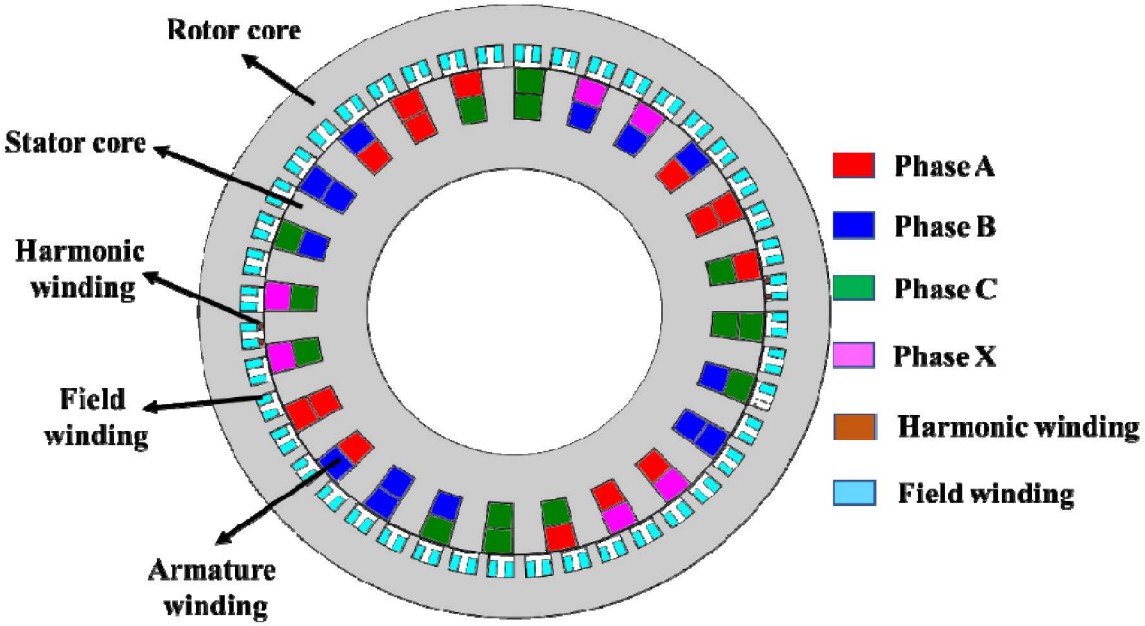

FIGURE 6. Machine used for the proposed self-excited brush-less WFVM topology.

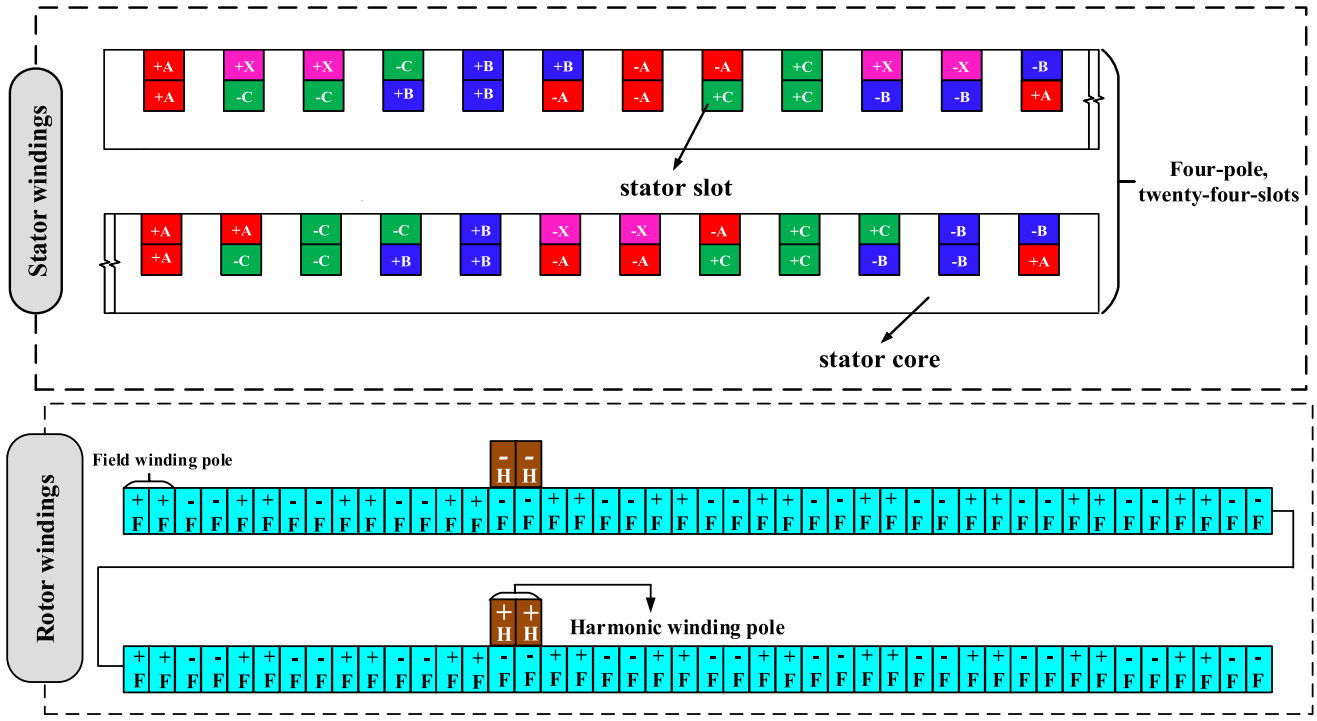

FIGURE 7. Armature and rotor winding outlines used for the proposed self-excited brush-less WFVM topology.

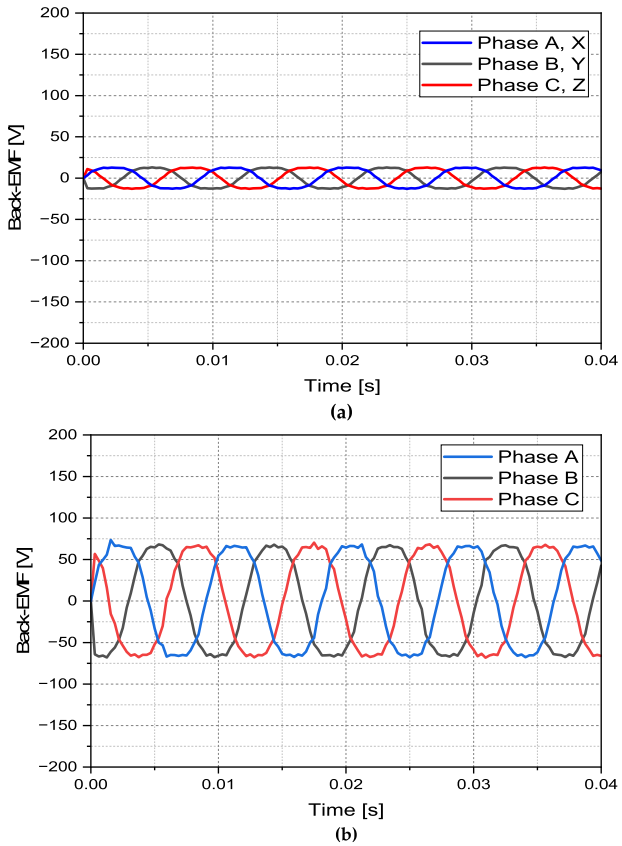

FIGURE 8. Back-EMF for (a) conventional and (b) proposed brush-less WFVM topologies.

injected current from current-controlled VSI, a four-pole main stator field and a two-pole pulsating sub-harmonic field are established in the airgap. The rotor is housed with harmonic and field windings connected in series by means of a full-bridge diode rectifier. The harmonic field will induce a current in the rotor harmonic winding, which will be rectified to energize the forty-four-pole rotor field winding to realize brush-less operation. The proposed brush-less WFVM topology is based on a single-inverter-outline, making it cost-effective and compact in comparison with the conventional sub-harmonic-based brush-less WFVM topology.

II. PROPOSED SELF-EXCITED BRUSHLESS WFVM TOPOLOGY AND ITS OPERATING PRINCIPLE

The proposed self-excited brush-less WFVM topology, as presented in Fig. 4, involves a four-pole main armature winding (ABC) and a two-pole excitation winding (X). Both windings are connected in series by means of an uncontrolled rectifier and are supplied current (I_{ABC}) from a single current-controlled VSI. This current is given by:

$$\left\{\begin{array}{l} I_A = I_p \cos \omega t \\ I_B = I_p \cos(\omega t - \frac{2\pi}{3}) \\ I_C = I_p \sin(\omega t + \frac{2\pi}{3}) \end{array}\right\} \quad (1)$$

where I_p denotes the peak value of the current and ω is used to represent the rotor angular speed.

The balanced three-phase currents injected to the ABC winding get rectified and simultaneously energize the two-pole excitation winding. This procedure results in a four-pole main stator MMF and a two-pole sub-harmonic MMF in the airgap. The four-pole MMF develops the main stator field; however, the two-pole sub-harmonic MMF develops the

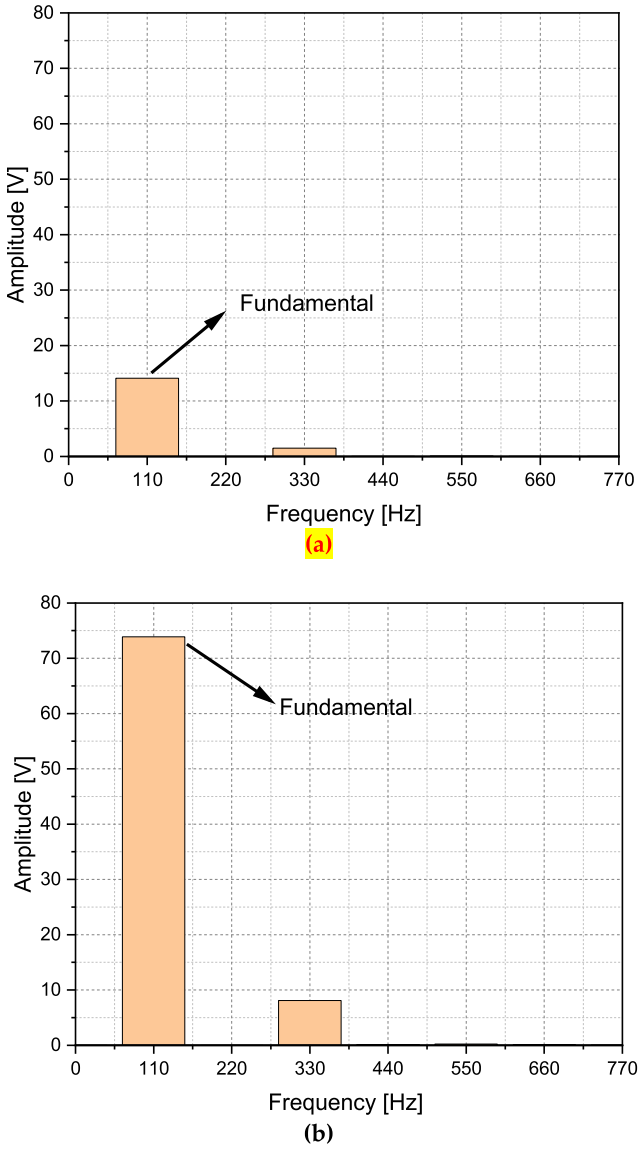

FIGURE 9. Harmonic contents of the back-EMF of (a) conventional and (b) proposed brush-less WFVM topologies.

harmonic field which is pulsating. The generated fields are presented in Fig. 5 and can be represented mathematically through equation (2):

$$F = \frac{3N_a}{2\pi} I_p \cos(\omega t - \theta) + \frac{3N_e}{2\pi} I_X \cos(\frac{\theta}{2}) \tag{2}$$

where F is the airgap flux, N_a is used to denote the ABC winding turns per phase, N_e represents the excitation winding (X) turns, and I_X is the excitation winding current [24], [25].

The rotor is altered to house the harmonic and field windings. As the developed magnetic fields are not synchronized because of the different number of poles, the harmonic field will be intercepted by the harmonic winding, which has an equal number of poles and induces a current in it. The induced current in the harmonic winding will be rectified by means of a full-bridge rectifier to energize the rotor field winding. For a vernier machine, the proper combination of stator slots, stator pole pairs, and rotor field winding pole pairs is required, and

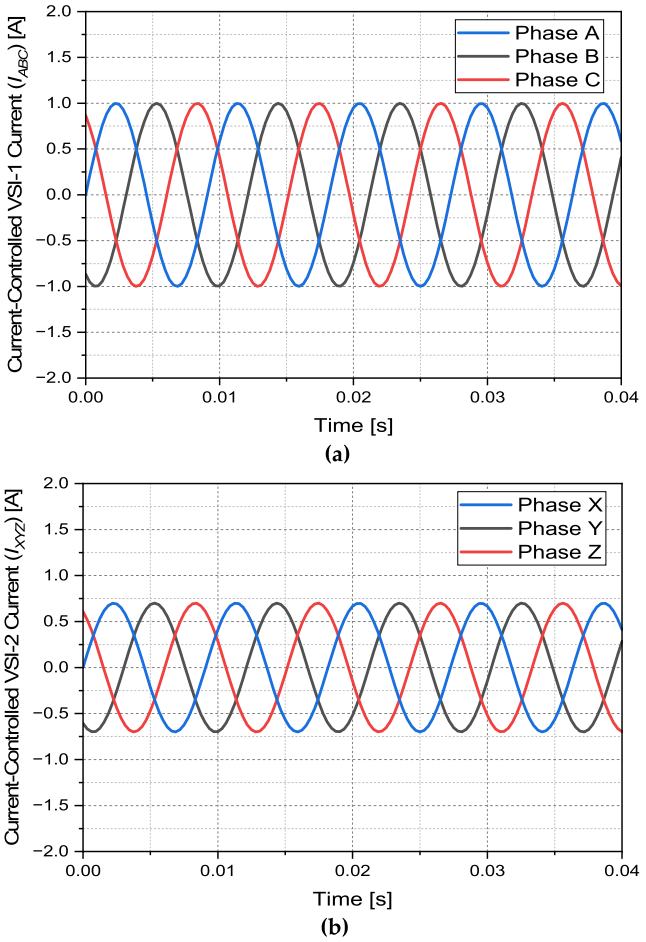

FIGURE 10. Armature currents for (a) ABC winding and (b) XYZ winding.

the machine must satisfy the following equation (3) to work in the vernier mode:

$$P_r = N_s \pm P_s \tag{3}$$

where P_r denotes the rotor field winding pole pairs, N_s is used to represent the stator slots number, and P_s denotes the stator pole pairs.

For the proposed self-excited brush-less WFSM topology, a four-pole, twenty-four-slot outer-rotor machine is used. To satisfy equation (3), the number of rotor field winding poles is kept at forty-four.

The main reason behind using an outer-rotor vernier machine to implement the proposed brush-less topology is its suitability for various applications such as in-wheel motors and washing machines. In addition, it offers a greater slot area for the rotor field winding poles, which helps avoid manufacturing complications associated with many rotor poles for the inner-rotor vernier machines. The speed of the vernier machine can be calculated using equation (4):

$$\frac{\omega_r}{\omega_{MMF}} = \frac{\text{rotor speed}}{\text{stator field speed}} = \frac{P_s}{P_r} \tag{4}$$

where ω_r denotes the rotor speed, and ω_{MMF} represents the main stator field speed [26], [27].

TABLE 1. Design specifications.

Attribute	Conventional Topology	Proposed Topology
Rated power	1.5 kW	1.5 kW
Stator outer diameter	238 mm	238 mm
Shaft diameter	140 mm	140 mm
Airgap	0.5 mm	0.5 mm
Rotor inner/outer diameter	239 mm/300 mm	239 mm/300 mm
Stator poles/slots	4/24	4/24
Rotor slots	44	44
ABC winding turns (N_a)	270	270
XYZ winding turns	270	-
X winding turns (N_e)	-	8
Harmonic/field winding turns	8/36	8/36
Stack length	30 mm	30 mm

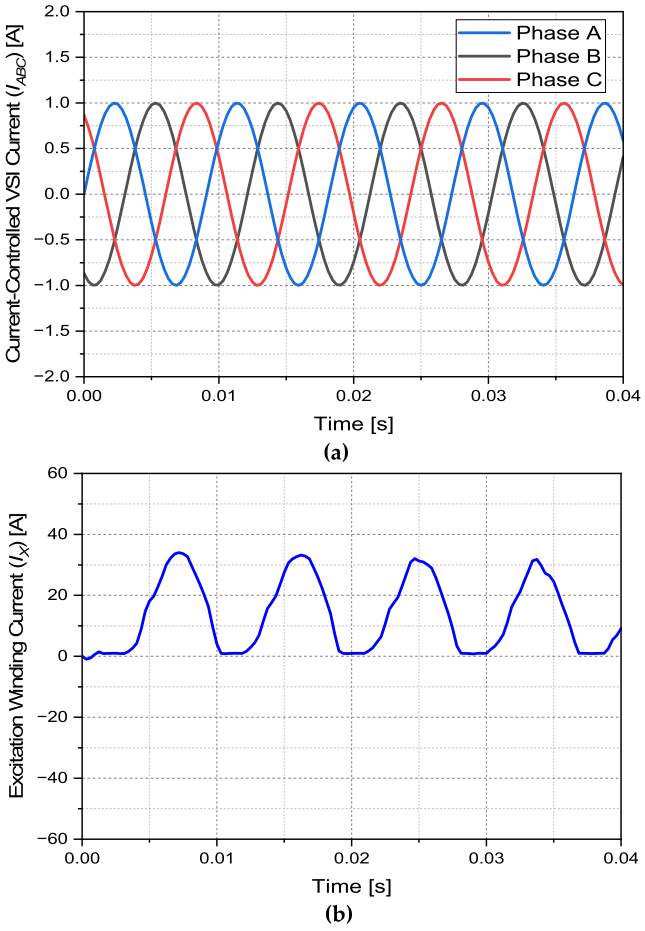

FIGURE 11. Armature currents for (a) ABC winding and (b) X winding.

The employed machine and the stator and rotor winding outlines are presented in Fig. 6 and 7, respectively. It can be seen from these figures that six slots in the twenty-four-slot machine are partially filled with the ABC winding. These partially filled slots are used to inset the excitation winding (X) in such a manner that the initial three slots are occupied with a positive excitation winding terminal represented by "+X", and the final three slots are housed with a negative terminal of the excitation winding that is represented by "-X". This resultantly generates a two-pole flux in the airgap through 360 mechanical degrees, as presented in the blue color waveform of Fig. 5. The ABC winding is coiled in a distributed manner, which results in a four-pole airgap flux as shown in the red waveform in Fig. 5.

III. ELECTROMAGNETIC ANALYSIS

For the operational validation of the conventional and proposed brush-less WFVM topologies and to realize their electromagnetic performance for the comparative performance analysis, two-dimensional machine models, as shown in Fig. 2 and 6, are developed in JMAG-Designer. The designing parameters of these machines are presented in Table. 1.

A. NO-LOAD ANALYSIS

To study the behavior of the conventional and proposed brush-less WFVM topologies under no-load conditions, no-load analysis is implemented in JMAG-Designer. Both machines are operated at 300 rpm, and their field winding is energized with a direct current of 1 A. The generated back-EMF of the conventional and proposed WFVMs are shown in Fig. 8(a) and (b), respectively. These figures illustrate that the magnitude of back-EMF for the ABC and XYZ windings of the conventional topology is around 10.003 V_{rms}; however, this magnitude for the proposed topology is 52.443 V_{rms}. The lower magnitude of the back-EMF for the conventional topology is due to the split of armature winding in two-halves. The harmonic contents of the generated back-EMF are presented in Fig. 9. From this result, the total harmonic distortion (THD) of the back-EMF for the conventional brush-less WFVM topology is calculated as 10.92%, whereas in the proposed self-excited brush-less WFVM topology, the THD for the back-EMF is around 11.33% which is 0.412% higher than the conventional topology. As the THD of the back-EMF under no-load conditions affects the torque ripple of the machine, the proposed brush-less WFVM topology will exhibit a higher magnitude

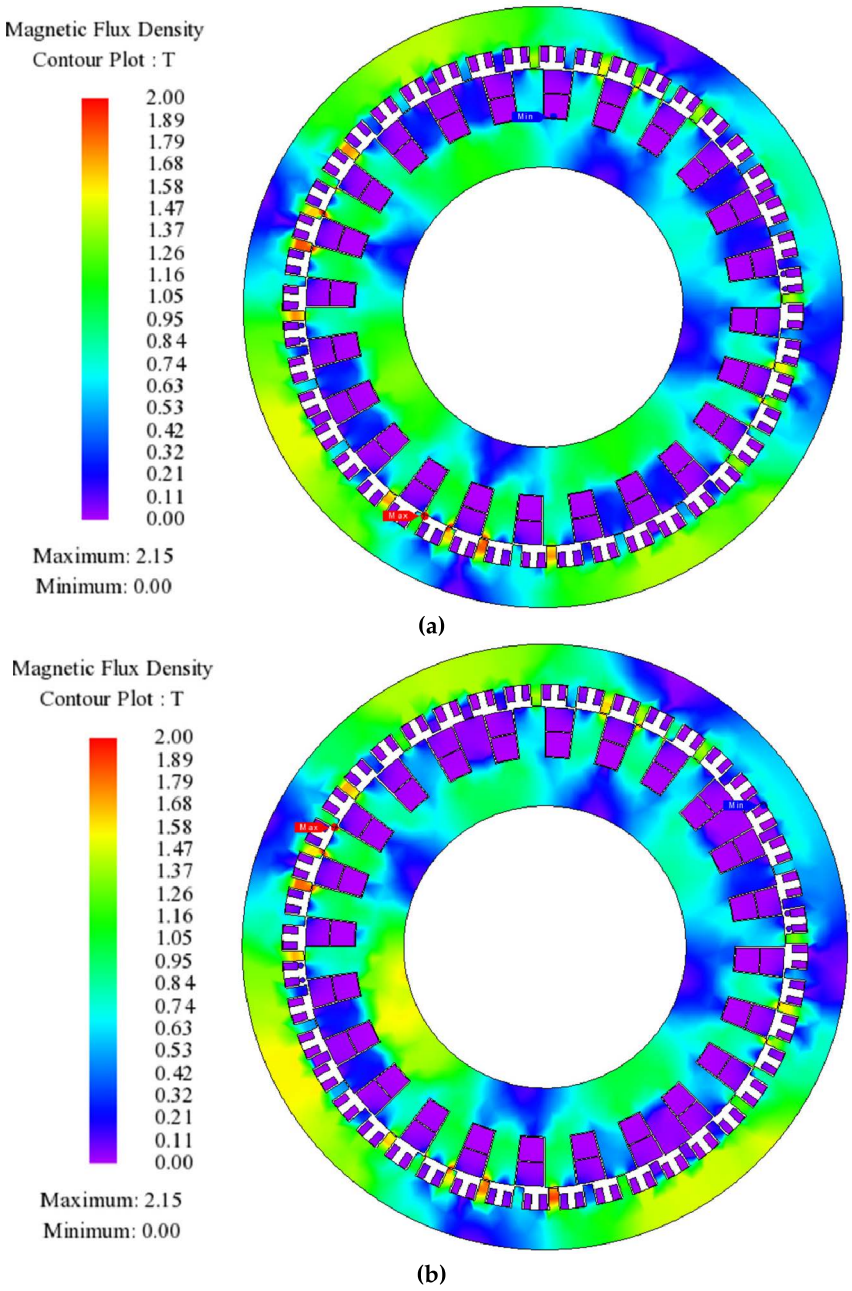

FIGURE 12. Magnetic field density graphs for (a) conventional and (b) proposed brush-less WFVMs.

TABLE 2. No-load performance comparison.

Attribute	Conventional Topology	Proposed Topology
Back-EMF (V_{rms})	10.003	52.443
THD (%)	10.92	11.33

of the torque ripple than the conventional WFVM topology. This will further be confirmed from the loaded analysis presented in section 3.2. The no-load results for the conventional and proposed brush-less WFVM topologies are presented in Table. 2.

B. LOADED ANALYSIS

For the loaded analysis of the conventional and proposed brush-less WFVM topologies, the shaft of the machines is rotated at a speed of 300 rpm, whereas the simulations of these machines are performed for 0.6 s. For the conventional

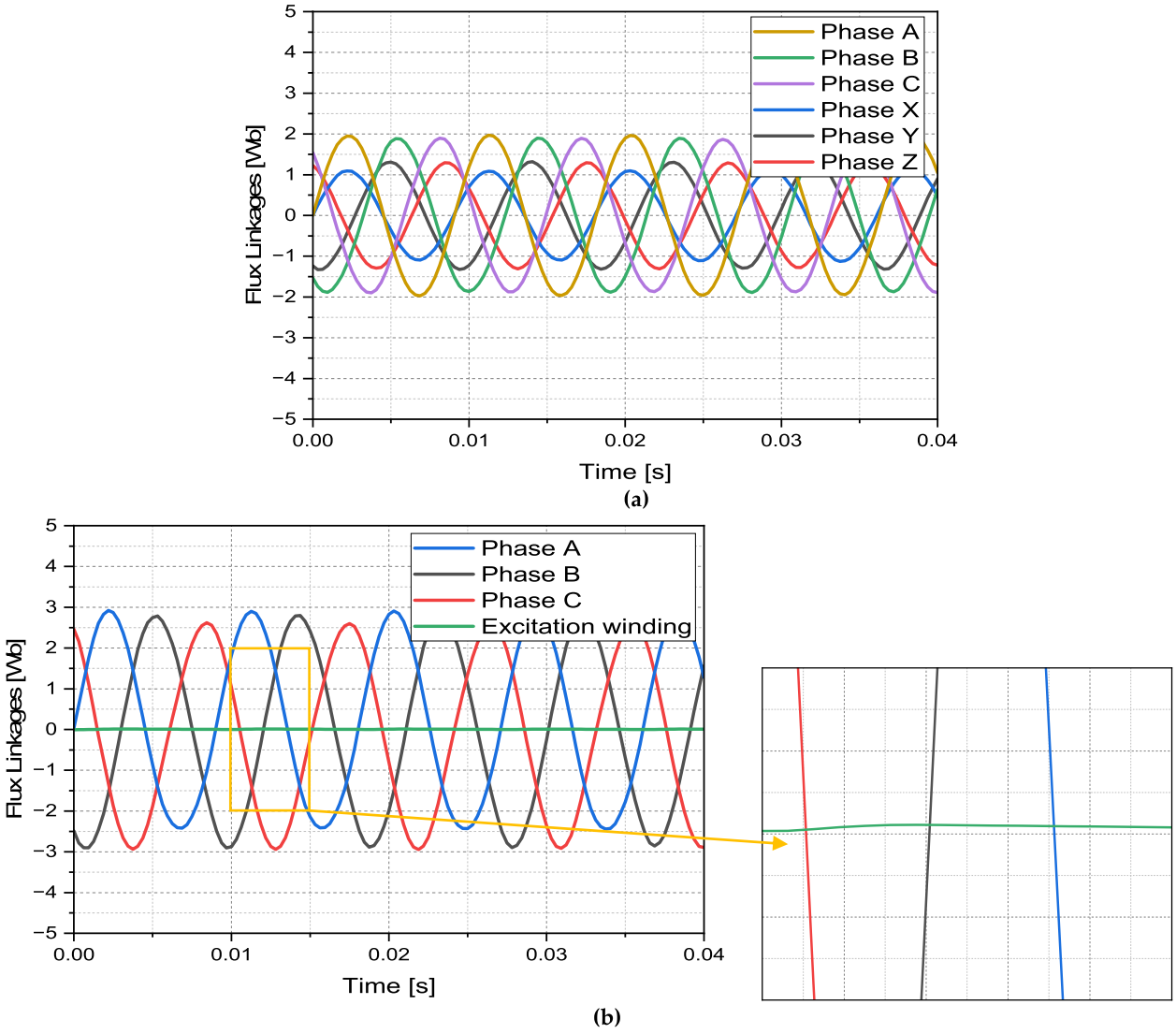

FIGURE 13. Flux linkages for (a) conventional and (b) proposed brush-less WFVM topologies.

TABLE 3. Performance comparison under loaded condition.

Attribute	Conventional Topology	Proposed Topology
Average Torque (Nm)	23.474	35.955
Torque Ripple (%)	41.53%	48.67
Total Iron Losses (W)	117.188	107.809
Total Copper Losses (W)	5.265	16.571
Total Losses (W)	239.641	232.191
Output Power (W)	747.457	1129.56
Efficiency (%)	75.75	82.94

brush-less topology, the input armature currents for ABC and XYZ windings are 1 A (peak) and 0.7 A (peak), respectively. These currents are injected at a frequency of 110 Hz. The input armature currents, *i.e.,* I_{ABC} and I_{XYZ} for the conventional brush-less topology, are presented in Fig. 10. For the proposed self-excited brush-less WFVM topology, the input armature winding current for ABC winding is 1 A (peak) supplied from the current-controlled VSI at a frequency of 110 Hz. This current is rectified through an un-controlled rectifier to energize the excitation winding (X). The magnitude of the rectified current (I_X) is around 17.35 A. The main armature winding and excitation winding currents, *i.e.,* I_{ABC} and $I_{X,}$ are shown in Fig. 11. These currents develop four-pole and two-pole magnetic fields in the machines' airgap

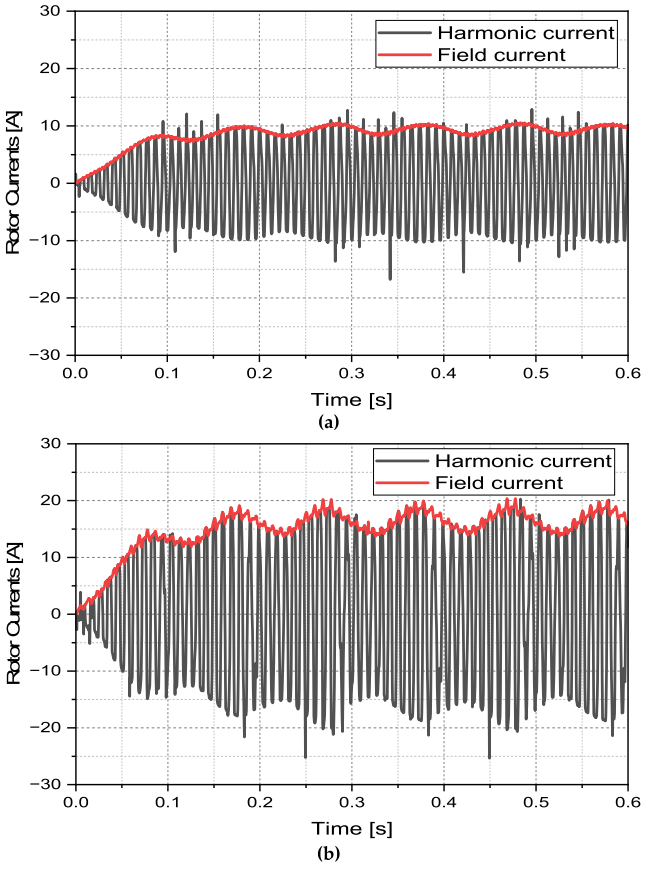

FIGURE 14. Rotor currents for (a) conventional and (b) proposed brush-less WFVM topologies.

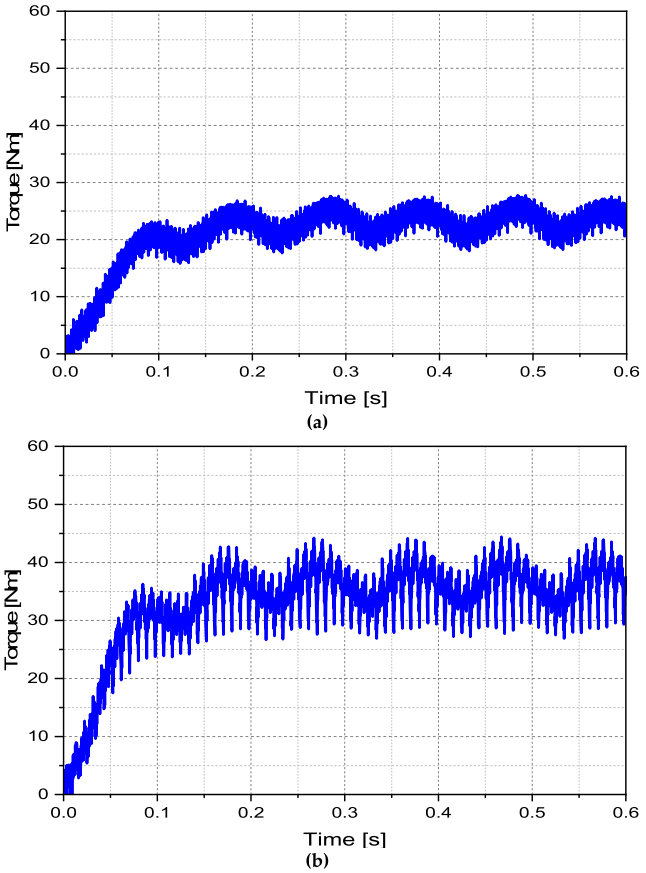

FIGURE 15. Output torque for (a) conventional and (b) proposed brush-less WFVMs.

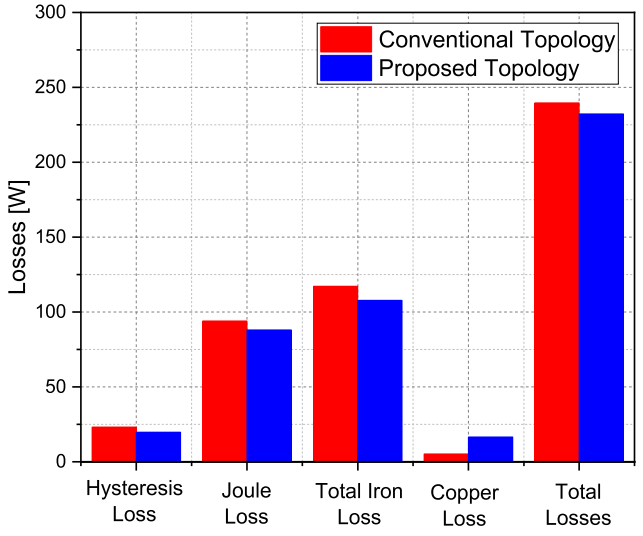

FIGURE 16. Losses for the conventional and proposed brush-less WFVM topologies.

to confirm the conventional and proposed brush-less WFVM topologies. Fig. 12 shows the flux density graphs of the machines, whereas the flux linkages for the conventional and proposed brush-less WFVMs are shown in Fig. 13.

The two-pole magnetic field induces a current in the harmonic winding, which is rectified to generate the rotor field. The magnetic interaction of the four-pole stator and forty-four-pole rotor fields produces torque through the electro-magnetic gearing phenomenon. Fig. 14 shows the induced harmonic and rectified field currents, whereas the developed torque for the conventional and proposed brush-less WFVM topologies is presented in Fig. 15. This figure shows that for the conventional brush-less WFVM topology, the magnitude of the average output torque is 23.474 Nm with a ripple of 41.53% under the steady-state operating condition. On the other hand, the magnitude of the average output torque for the proposed self-excited brush-less WFVM topology is around 35.955 Nm, with a ripple of 48.67%. This result shows that, unlike the conventional brush-less WFVM topology, which requires a dual-inverter-outline, the proposed single-inverter-controlled brush-less WFVM topology produces 34.71% more average output torque in comparison with the conventional topology. On the other hand, a slight increase in the torque ripple of around 7.14% is observed for the proposed topology, which may be avoided through parametric optimization of the machine topology.

To calculate the efficiency of the conventional and proposed brush-less WFVM topologies, loss studies for the stator and rotor cores of the employed machines are implemented in JMAG-Designer. Fig. 16 presents the total calculated losses (iron and copper) for the conventional and proposed brush-less WFVM topologies. These calculations

show that the total magnitude of losses for the conventional topology is around 239.641 W, whereas the magnitude for the proposed topology is 232.191 W. The output power of the conventional and proposed brush-less WFVM topologies are 747.457 W and 1129.56 W, respectively. This results in 75.75 % efficiency for the conventional topology and 82.94% efficiency for the proposed self-excited brush-less WFVM topology. These results are presented in Table. 3.

IV. CONCLUSION

A self-excited brush-less WFVM topology based on a single-inverter-outline was proposed in this paper. The proposed topology used a four-pole main stator winding and a two-pole excitation winding connected through an un-controlled rectifier. This procedure developed a four-pole main stator field and a two-pole sub-harmonic field as the current is injected from a single current-controlled VSI to the main stator winding. The sub-harmonic field was used to induce a current in the harmonic winding, which was rectified to energize forty-four-pole rotor field winding to realize brush-less operation. The proposed topology was implemented in FEA using a four-pole, twenty-four-slot machine and compared with the conventional sub-harmonic-based brush-less WFVM topology under the same loading and operating conditions. The results showed that the proposed topology generates 34.71% more average output torque than the conventional topology. The total losses of the proposed topology are calculated as 232.191 W, which is 3.2% lower than the total calculated losses of the conventional topology. The efficiency of the proposed topology was found to be 7.19% higher than the conventional one.

On the other hand, a slightly higher magnitude of torque ripple of 7.14% is observed for the proposed topology, which may be addressed while considering the parametric optimization of the machine. The proposed brush-less WFVM topology performed well under no-load conditions as well. It generated 42.44 V_{rms} more back-EMF in comparison with the conventional topology.

From the results, it can be determined that the proposed self-excited brush-less WFVM topology could be a cost-effective, compact, and high-performing (in terms of average torque, total losses, and efficiency) alternative to the conventional brushed and brush-less WFVM topologies.

REFERENCES

[1] W. Li, T. W. Ching, K. T. Chau, and C. H. T. Lee, "A superconducting Vernier motor for electric ship propulsion," *IEEE Trans. Appl. Supercond.*, vol. 28, no. 3, pp. 1–6, Apr. 2018.
[2] S. Jia, R. Qu, and J. Li, "Analysis of the power factor of stator DC-excited Vernier reluctance machines," *IEEE Trans. Magn.*, vol. 51, no. 11, pp. 1–4, Nov. 2015.
[3] N. Baloch, S. Atiq, and B.-I. Kwon, "A wound-field pole-changing Vernier machine for electric vehicles," *IEEE Access*, vol. 8, pp. 91865–91875, 2020.
[4] F. Wu and A. M. EL-Refaie, "Permanent magnet Vernier machines: A review," in *Proc. 13th Int. Conf. Electr. Mach. (ICEM)*, 2018, pp. 372–378.
[5] K. Kiyota, H. Sugimoto, and A. Chiba, "Comparing electric motors: An analysis using four standard driving schedules," *IEEE Ind. Appl. Mag.*, vol. 20, no. 4, pp. 12–20, Jul. 2014.
[6] S. S. H. Bukhari, J. Yu, M. A. Shah, M. Bajaj, and J. Ro, "Novel sub-harmonic-based self-excited brushless wound rotor synchronous machine," *IEEE Can. J. Electr. Comput. Eng.*, vol. 45, 2022.
[7] M. Ayub, A. Hussain, G. Jawad, and B.-I. Kwon, "Brushless operation of a wound-field synchronous machine using a novel winding scheme," *IEEE Trans. Magn.*, vol. 55, no. 6, pp. 1–4, Jun. 2019.
[8] S. S. H. Bukhari, J. Yu, M. A. Shah, M. Bajaj, and J. Ro, "Brushless wound rotor synchronous machine based on consequent-pole rotor structure with better torque attributes," *Int. Trans. Electr. Energy Syst.*, vol. 2022, Jun. 2022, Art. no. 6289596.
[9] A. Hussain and B. I. Kwon, "A new brushless wound rotor synchronous machine using a special stator winding arrangement," *Elect. Eng.*, vol. 100, no. 3, pp. 1797–1804, Sep. 2018.
[10] S. S. H. Bukhari, H. Ahmad, F. A. Chachar, and J. Ro, "Brushless field-excitation method for wound-rotor synchronous machines," *Int. Trans. Electr. Energy Syst.*, vol. 31, no. 8, Aug. 2021, Art. no. e12961.
[11] A. Hussain, S. Atiq, and B. I. Kwon, "Optimal design and experimental verification of wound rotor synchronous machine using subharmonic excitation for brushless operation," *Energies*, vol. 11, no. 3, p. 554, 2018.
[12] S. S. H. Bukhari, G. J. Sirewal, F. A. Chachar, and J. Ro, "Dual-inverter-controlled brushless operation of wound rotor synchronous machines based on an open-winding pattern," *Energies*, vol. 13, no. 9, p. 2205, 2020.
[13] F. Yao, Q. An, L. Sun, and T. A. Lipo, "Performance investigation of a brushless synchronous machine with additional harmonic field windings," *IEEE Trans. Ind. Electron.*, vol. 63, no. 11, pp. 6756–6766, Nov. 2016.
[14] G. J. Sirewal, M. Ayub, and B.-I. Kwon, "A self-excitation scheme for a brushless synchronous generator," in *Proc. 10th Int. Conf. Power Electron. ECCE Asia (ICPE-ECCE Asia)*, Busan, South Korea, May 2019, pp. 1227–1232.
[15] F. Yao, Q. An, X. Gao, L. Sun, and T. A. Lipo, "Principle of operation and performance of a synchronous machine employing a new harmonic excitation scheme," *IEEE Trans. Ind. Appl.*, vol. 51, no. 5, pp. 3890–3898, Oct. 2015.
[16] Q. Ali, T. A. Lipo, and B.-I. Kwon, "Design and analysis of a novel brushless wound rotor synchronous machine," *IEEE Trans. Magn.*, vol. 51, no. 11, pp. 1–4, Nov. 2015.
[17] F. Yao, D. Sun, L. Sun, and T. A. Lipo, "Dual third-harmonic-current excitation principle of a brushless synchronous machine based on double three-phase armature windings," in *Proc. 22nd Int. Conf. Electr. Mach. Syst. (ICEMS)*, Harbin, China, Aug. 2019, pp. 1–4.
[18] K. Inoue, H. Yamashita, E. Nakamae, and T. Fujikawa, "A brushless self-exciting three-phase synchronous generator utilizing the 5th-space harmonic component of magneto motive force through armature currents," *IEEE Trans. Energy Convers.*, vol. 7, no. 3, pp. 517–524, Sep. 1992.
[19] Q. Ali, A. Hussain, N. Baloch, and B.-I. Kwon, "Design and optimization of a brushless wound-rotor Vernier machine," *Energies*, vol. 11, no. 2, p. 317, 2018.
[20] Q. Ali, S. S. H. Bukhari, and S. Atiq, "Variable-speed, sub-harmonically excited BL-WRSM avoiding unbalanced radial force," *Electr. Eng.*, vol. 101, no. 1, pp. 251–257, 2019.
[21] S. S. H. Bukhari, G. J. Sirewal, M. Ayub, and J. Ro, "A new small-scale self-excited wound rotor synchronous motor topology," *IEEE Trans. Magn.*, vol. 57, no. 2, pp. 1–5, Feb. 2021.
[22] S. S. H. Bukhari, Q. Ali, J. D. Gandoy, and J. Ro, "High-efficient brushless wound rotor synchronous machine topology based on sub-harmonic field-excitation technique," *Energies*, vol. 14, no. 15, p. 4427, 2021.
[23] S. S. H. Bukhari, H. Ahmad, G. J. Sirewal, and J. Ro, "Simplified brushless wound field synchronous machine topology based on a three-phase rectifier," *IEEE Access*, vol. 9, pp. 8637–8648, 2021.
[24] G. Dajaku and D. Gerling, "New self-excited synchronous machine with tooth concentrated winding," in *Proc. 3rd Int. Electr. Drives Prod. Conf. (EDPC)*, Nüremberg, Germany, Oct. 2013, pp. 29–30.
[25] B. Kim and T. A. Lipo, "Operation and design principles of a PM Vernier motor," *IEEE Trans. Ind. Appl.*, vol. 50, no. 6, pp. 3656–3663, Dec. 2014.
[26] B. Kim, "Characteristic analysis of a Vernier PM motor considering adjustable speed control," in *Proc. IEEE Conf. Expo. Transp. Electrific. Asia–Pacific (ITEC Asia–Pacific)*, Busan, South Korea, Jun. 2016, pp. 1–4.
[27] M. Bilal, J. Ikram, A. Fida, S. S. H. Bukhari, N. Haider, and J. Ro, "Performance improvement of dual stator axial flux spoke type permanent magnet Vernier machine," *IEEE Access*, vol. 9, pp. 64179–64188, 2021.